 ISBN 978-3-8007-3343-9 © VDE VERLAG GMBH

Energy Efficient Supply of WSN Nodes using Component-Aware Dynamic Voltage Scaling

Leander B. Hörmann, Philipp M. Glatz, Christian Steger and Reinhold Weiss
Institute for Technical Informatics
Graz University of Technology
Graz, Austria
Email: {Leander.Hoermann@, Philipp.Glatz@, Steger@, RWeiss@}TUGraz.at

***Abstract*—Energy efficiency is very important for wireless sensor networks (WSNs), because the consumable energy is limited. Each WSN node has its own power supply. The lifetime of the WSN node depends basically on its average power consumption. Therefore, an efficient supply of the WSN node can enhance the lifetime of it. Typically, the various components of a WSN node (microcontroller, transceiver, sensors) have different supply voltage ranges. To save as much energy as possible, the supply voltage of the node should be as low as possible. Therefore, a voltage converter is needed to reduce the voltage of a battery. The minimum allowed supply voltage depends on the components that are active. The active components and consequently the minimum allowed supply voltage vary over time. Component-aware dynamic voltage scaling (CADVS) can be used to adapt the supply voltage of the node. This work presents the possible energy savings using four different voltage conversion techniques. It has been shown that CADVS can be used to save up to 31.5 % of the energy compared to a constant voltage supply using the introduced scenario while achieving the same end-user performance.**

I. Introduction

Wireless sensor networks (WSNs) are very power critical systems. They are used to measure physical quantities and transmit the information of its environment through the network in application areas with mobility or bad infrastructure. A WSN typically consists of a lot of sensor nodes. Each sensor node is an intelligent device which is responsible to forward messages through the network and to prepare the measured data for the transmission. These tasks are typically fulfilled by a microcontroller. The missing wired infrastructure causes the need of dedicated energy sources for each sensor node. Conventional batteries are cheap and provide a reliable supply for a certain period of time, because each battery has a limited capacity. Therefore, the lifetime of battery powered sensor nodes is also limited. Energy harvesting systems (EHSs) can be used to extend the lifetime of the sensor nodes [1]–[3]. They utilize environmental energy sources. Energy harvesting devices (EHDs) convert the energy of the environmental sources into electrical energy. Typical EHDs are solar cells and thermogenerators. The converted energy must be stored, because *energy from the environment is generally unpredictable, discontinuous, and unstable* [4]. The available energy is often very low compared to the energy consumption of the sensor node. These are the reasons of the strict power constraints for WSNs.

The application areas of WSNs are manifold. Precision agriculture [5], [6], wildlife monitoring [7], [8], human health care [9] and structural health monitoring [10] are only a few examples. Typically, a sensor node is adapted to its special application area. Therefore, only the necessary sensors and components are embedded into the sensor node and significant energy can be saved. The needed sensors depend strongly on the application area and are often predetermined. Each sensor has its own power requirements and its own supply voltage range. Therefore, the components (especially the microcontroller) have to be adapted to the sensors to ensure proper functionality. In many cases, the supply voltage of the sensor node is set to a fixed high value, because only one component of the node needs this high voltage. The other components do not need such a high supply voltage. Therefore, lot of energy is wasted, because of a single component.

Another case of wasting energy is the direct connection of the sensor node to the energy storage unit (ESU), e.g. battery. The voltage of almost all ESUs depends on its energy level. Typically, the voltage decreases with decreasing energy level of the ESU. Each sensor node has a specific supply voltage range wherein a proper functionality is guaranteed. Below the lower limit the sensor node cuts out. Therefore, the voltage of the fully charged ESU must be higher than this lower limit. The emerging difference is wasted energy. This difference depends on the lower limit of the supply range and the type of the ESU.

Component-aware dynamic voltage scaling (CADVS) can be used to close the gap between the different minimal supply voltages of the different sensors and components. The rest of the paper is organized as follows: Section II discusses related work. Section III describes the principals of energy efficient supply of WSN nodes and CADVS applied to the nodes. Section IV shows the possible gains using DVS. Finally, Section V concludes the paper and shows directions for future work.

II. Related Work

As mentioned before, WSN nodes are often supplied by conventional batteries. The problem is the limited lifetime. It can be extended by reducing the power consumption of the sensor node. However, this extension is limited by the leakage currents of each battery. Figure 1 shows the expected

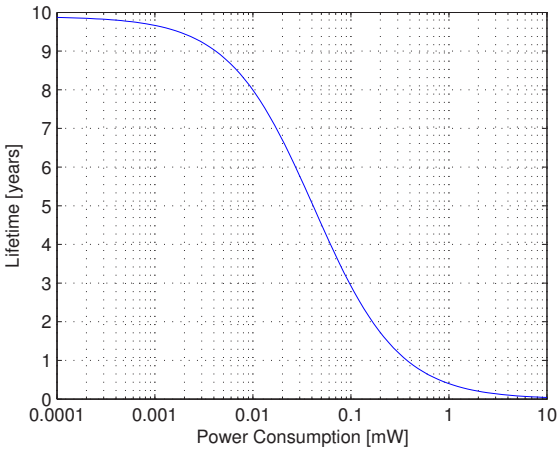

Fig. 1. Lifetime of a battery-powered system versus average power consumption using a simple battery model of a single AA cell (NiMH) with 2.6 Ah and a leakage current of 30 μA [11].

lifetime of a single AA cell (NiMH) with a capacity of 2.6 Ah depending on the current consumption of the sensor node. A typical leakage current of such a cell is 30 μA [11]. Therefore, the batteries have to be replaced after a certain period of time. This is called battery replacement problem as mentioned in [12]. The replacement is sometimes very difficult, because the WSN nodes are deployed at hard-to-access locations. Hence, the replacement should be avoided if possible.

An EHS can extend the lifetime of a WSN node by utilizing environmental energy sources. A theoretical energy harvesting model is introduced in [13]. The model deals with the description of environmental energy sources and the energy sink (consumer). It consists of a so called (ρ, σ_1, σ_2) - source and a (ρ', σ) - consumer. The (ρ, σ_1, σ_2) - source is used to describe environmental energy sources. $P(t)$ is the continuous power output of the source at the time t. ρ is the average power output of this source. σ_1 and σ_2 describe the changes of the power output. The power consumption is also characterized with the average power consumption ρ' and the maximum power consumption σ. It is called (ρ', σ) - consumer. The following theorem has been proven in [13]:
Sustainable Performance at Eternity (Variable Consumption Profile): If a (ρ', σ) - consumer device is powered by a (ρ, σ_1, σ_2) - source model, has an energy storage capacity of $\sigma + \sigma_1 + \sigma_2$, and $\rho' < \rho$, then the device can operate forever.

Two conclusions can be derived from this model. First, the EHS needs a buffer (ESU) to bridge the discontinuous power output of the environmental energy source. There are different types of ESUs that can be used, e.g. rechargeable batteries (nickel-cadmium NiCd, nickel-metal hydride NiMH, lithium ion LiIon or lithium-ion polymer LiPo) or double layer capacitors (DLCs). Second, if the average power consumption of the WSN node is lower than the average harvested power of the environmental energy source and the ESU is well dimensioned, then a perpetual operation is possible. This solves the battery replacement problem.

TABLE I
POWER DENSITIES OF DIFFERENT HARVESTING TECHNOLOGIES [2], [14].

Harvesting technology	Power density
Solar cells (outdoor at noon)	10-15 mW/cm^2
Solar cells (indoor) [15]	$\approx 10\,\mu W/cm^2$
Piezoelectric (shoe inserts)	$\approx 300\,\mu W/cm^3$
Vibration (small microwave oven)	$\approx 100\,\mu W/cm^3$
Thermoelectric ($10°C$ gradient)	$\approx 40\,\mu W/cm^3$
Acoustic noise (100dB)	$\approx 1\,\mu W/cm^3$

The amount of harvestable energy depends on the type of the environmental energy source, on the power of the energy source and on the efficiency of the EHD. Table I shows a list of commonly used energy harvesting technologies and their power densities [2], [14]. It can be seen that the power density of the solar cell depends dramatically on the location. If the EHS is deployed outdoor, solar cells have the best power density. Therefore, the power consumption of the WSN node must be lower or the size of the EHD must be increased.

Dynamic voltage scaling (DVS) is commonly used to adapt the supply voltage of a processor depending on its clock frequency. The clock frequency can be reduced if the workload of the processor is low. In [16] the design issues for DVS are explained. In [17] they describe various algorithms that can be used for DVS. These algorithms *reduce energy consumption by changing processor speed and voltage at run-time depending on the needs of the applications running* [17]. In [18] DVS is applied to low power microprocessors. They use a low power StrongARM embedded Linux platform running a multimedia application for evaluation. In [19] they describe the energy savings using dynamic frequency and voltage scaling. The reduction of the frequency causes linear energy savings. Additionally, the adaption of the supply voltage to the lower clock frequency of the processor causes quadratic energy savings. However, all the works only consider the power consumption of the processor core itself. Other components are not included in their calculations. In [20] they have implemented a dynamic voltage and frequency scaling platform using an MSP430 ultra-low power microcontroller from Texas Instruments and other components of the shelf (COTS). This approach is very interesting, because they can vary the supply voltage of the MSP430 microcontroller. However, they do not consider the efficiency and the leakage currents of the voltage converter. The following section describes CADVS applied on the whole sensor node and the influence of the voltage converters.

III. Energy Efficient Supply of WSN Nodes

This section starts with the basics of the energy efficient supply of WSN nodes. Then, the scenario that is used for the calculations is explained in detail. Afterwards, two different voltage converters and their theoretical savings are discussed. Finally, CADVS and the possible energy savings are explained.

As mentioned in the introduction, an energy efficient supply of a WSN node is very important and can extend the lifetime of such a node. Each sensor node typically consists of a

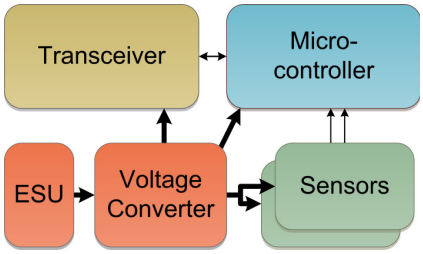

Fig. 2. Structure of a wireless sensor node (extended from [21]).

microcontroller and some sensors. To guarantee an efficient supply of the WSN node a conversion circuit is needed. Typically, this converter reduces the battery voltage to a constant value. Figure 2 shows the structure of a wireless sensor node. The converter is placed between the ESU (e.g. a battery or a DLC) and the rest of the sensor node. Usually, the whole sensor node is supplied by the same voltage. Multiple supply voltages are possible, but dramatically increase the complexity of the hardware, because each voltage level needs its own converter and between each voltage level some level shifter hardware is needed. Therefore, it is not useful to supply a sensor node with different voltage levels simultaneously in general.

Energy can be saved by switching off the components which are not needed currently by the application. This means the power supply of each component should be controllable by the microcontroller. Then, the driver software of a component or the application software itself can enable or disable the specific components. Therefore, a program or a part of a program has a list of the used hardware components L. The only component which is supplied all the time is the microcontroller. Hence it is always on the list L. The rest of the list depends on the components that are currently needed by the application (transceiver, sensors). Each of the components has its own supply voltage range with a lower limit $V_{sup,min,component}$. This limit is the lowest possible supply voltage (LPSV) of a component. The list L and the LPSVs $V_{sup,min,component}$ of the components result in a list of the LPSVs L_{LPSV}. Due to the fact that all hardware components of a sensor node are supplied by the same voltage, the minimum allowed voltage can be determined as shown in Equation 1.

$$V_{sup,min,node} = max(L_{LPSV}) \quad (1)$$

The list of the needed hardware components L depends on the application or even on the part of the application which is currently executed by the microcontroller. Therefore, the list changes over the time and consequently the list L_{LPSV} and the minimum allowed supply voltage $V_{sup,min,node}$. To be as efficient as possible, the supply voltage of the node should be equal to the minimum allowed supply voltage: $V_{CC} = V_{sup,min,node}$. This variation depends on the application and on the embedded hardware components of the mote. The following section describes the assumptions for further considerations.

TABLE II
HARDWARE COMPONENTS AND THEIR SUPPLY VOLTAGE RANGE.

Hardware Component	Supply Range	$V_{sup,min,component}$
Microcontroller	1.8 V to 3.6 V	1.8 V
Temperature Sensor	3.3 V to 3.3 V	3.3 V
Transceiver	2.4 V to 3.6 V	2.4 V

A. Scenario

A typical energy saving method used in WSNs is duty cycling (DC). The sensor nodes are only active for a short period of time t_{active}. During this time, the node collects the information of its environment, preprocesses the data and transmits these data. During the rest of the time t_{sleep}, the sensor node is placed into a sleep state to save as much energy as possible. Thus, one interval T consists of the active period t_{active} and the sleep period t_{sleep}.

An MSP430F1611 from Texas Instruments is used as microcontroller. This microcontroller has a supply voltage range from 1.8 V to 3.6 V [22]. To be able to use the full supply range the clock frequency of the microcontroller has to be limited to 4 MHz. The active mode current I_{AM} is calculated according to the datasheet. First, the current consumption at a clock frequency of 1 MHz and the given supply voltage V_{CC} is calculated as shown in Equation 2. Therefore, the current consumption at 1 MHz and 3 V is used ($I_{AM,1MHz,3V} = 500\,\mu$A). Then, the current consumption at the given clock frequency f can be calculated as shown in Equation 3).

$$I_{AM,1MHz}(V_{CC}) = I_{AM,1MHz,3V} + 210\,\mu\text{A/V} \cdot (V_{CC} - 3\,\text{V}) \quad (2)$$

$$I_{AM}(V_{CC}, f) = I_{AM,1MHz}(V_{CC}) \cdot f[\text{MHz}] \quad (3)$$

The sleep mode current I_{sleep} (low power mode 3, only the 32 kHz timer is active) is interpolated using the two values given in the datasheet [22] (Equation 4).

$$I_{sleep}(V_{CC}) = 1.3\,\mu\text{A} \cdot (V_{CC} - 2.2\,\text{V}) \cdot \frac{2.6\,\mu\text{A} - 1.3\,\mu\text{A}}{3\,\text{V} - 2.2\,\text{V}} \quad (4)$$

The WSN node should be used to measure the temperature of the environment. Therefore, the precise temperature sensor TMP05B from Analog Devices is embedded. It has a typical accuracy of 0.2 % if the supply voltage is in the range of 3.135 V to 3.465 V [23]. The full supply voltage range is from 3.0 V to 5.5 V. However, to guarantee the best accuracy, the supply voltage of the temperature sensor should be 3.3 V. Furthermore, the sensor node uses the MRF24J40MB 2.4 GHz IEEE802.15.4 transceiver module from Microchip. It has a supply voltage range from 2.4 V to 3.6 V [24]. Table II summarizes the embedded components and their supply voltage ranges.

Furthermore, it is assumed that the sensor node is in a sleep state (t_{sleep}) during 85 % of the interval T. Then the sensor node wakes up and performs some measurements (t_{meas}) during 5 %. After that, the measured data is preprocessed (t_{comp}) during 5 % of the interval. Therefore, no other hardware components are needed. Finally, the sensor node sends the

TABLE III
SUBINTERVALS AND THE NEEDED HARDWARE COMPONENTS.

Subinterval	Needed Components	$V_{sup,min,node}$
Sleep	Microcontroller	1.8 V
Active, Measurement	Microcontroller Temperature Sensor	3.3 V
Active, Computation	Microcontroller	1.8 V
Active, Communication	Microcontroller Transceiver	2.4 V

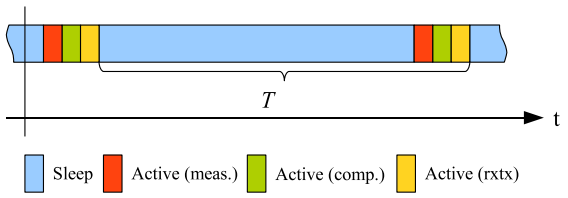

Fig. 3. Chronological sequence of an interval T.

results through the network (t_{comm}) during the last 5 % of the interval. The DC can be calculated according to Equation 5.

$$DC = \frac{t_{active}}{T} = \frac{t_{meas} + t_{comp} + t_{comm}}{T} \quad (5)$$

$$= \frac{15}{100} = 15\,\% \quad (6)$$

Table III shows the needed components of each part of the interval and the resulting minimum supply voltage of the node $V_{sup,min,node}$. Figure 3 shows the chronological sequence of the interval.

As shown in Fig. 2, a voltage converter is placed between the ESU and the components of the sensor node. The minimum supply voltage of the WSN node is 3.3 V and the maximum supply voltage is 3.6 V. This is a very small range and there is no battery type that operates well in this range. It would be possible to use a battery, which is not fully loaded but this would impair dramatically the usable capacity of the battery. Therefore, it is not possible to supply the node directly. The voltage converter reduces the battery voltage to a constant value. However, a little voltage drop $U_{drop,min}$ remains at the converter. The relation is shown in Equation 7.

$$U_{battery,min} = U_{drop,min} + U_{sup,node} \quad (7)$$

Therefore, the minimum voltage of battery $U_{battery,min}$ must be higher than the supply voltage of the node $U_{sup,node} = 3.3\,\text{V}$. For further calculations a minimum voltage drop of $U_{drop,min} = 0.2\,\text{V}$ of the converter is assumed [25], [26]. Table IV shows five possible battery types to supply the WSN node. All values are from [27]. The first column shows the type of the battery and the second column shows the number of needed cells which have to be connected in series to achieve the minimum supply voltage of the node. The third column lists the voltage values of the fully charged cell (or cells) and the fourth column shows the average voltage during a full discharge process. Finally, the last column shows the estimated usable capacity of the battery concerning the supply voltage

TABLE IV
POSSIBLE BATTERY TYPES FOR A SUPPLY OF THE WSN NODE [27].

Battery Type	Needed Cells	Start Voltage	Avg. Discharge Voltage	Usable Capacity
Alkaline	3	4.5 V	≈ 3.6 V	≈ 65 %
NiMH	3	4.14 V	≈ 3.75 V	≈ 89 %
NiCd	3	4.44 V	≈ 3.78 V	≈ 92 %
LiIon	1	4.1 V	≈ 3.76 V	≈ 95 %
LiPo	1	4.1 V	≈ 3.8 V	≈ 95 %

of the node and the minimum voltage drop of the converter. The minimum voltage of the battery is $U_{battery,min} = 3.5\,\text{V}$. The table shows that the LiIon and the LiPo rechargeable batteries have the best usable capacity. The alkaline battery is not rechargeable and is only given as reference. The low usable capacity is caused by the faster drop of the cell voltage compared to the other types.

B. Voltage Conversion Techniques

As mentioned before, energy can be saved if the voltage of the battery is reduced using a voltage converter. Basically, there are two different types of voltage converters which are explained in the following two sections.

1) Linear Voltage Regulators: This type provides a constant output voltage by adapting its internal resistance. So called low-dropout (LDO) regulators are linear voltage regulators which can operate with a low difference of the input and the output voltage.

Figure 4a shows the dependency of the current (blue trace) and the power consumption (red trace) of the microcontroller on the supply voltage during active mode at 4 MHz. The values are simulated using Equation 2. It is a linear dependency of the current consumption on the supply voltage. When using an LDO regulator, the difference between the battery voltage V_{Bat} and the supply voltage of the microcontroller V_{CC} drops at the regulator V_{LDO} (see Equation 8).

$$V_{Bat} = V_{LDO} + V_{CC} \quad (8)$$

The current through the microcontroller is equal to the current through the LDO (Equation 9).

$$I_{LDO} = I_{\mu C} \quad (9)$$

The power consumption of the microcontroller and the LDO can be calculated as shown in Equation 10.

$$P(V_{CC}) = I_{LDO} \cdot V_{Bat} \quad (10)$$

$$= I_{AM}(V_{CC}) \cdot V_{Bat}$$

It can be seen that the power consumption depends linearly on the supply voltage. The reason is that the input current of the LDO regulator is the same as the output current and therefore the current of the microcontroller.

Figure 4b shows the dependency of the current (blue trace) and the power consumption (red trace) of the microcontroller depending on the supply voltage during sleep mode (low power mode 3, only the 32 kHz timer is active). Due to the fact

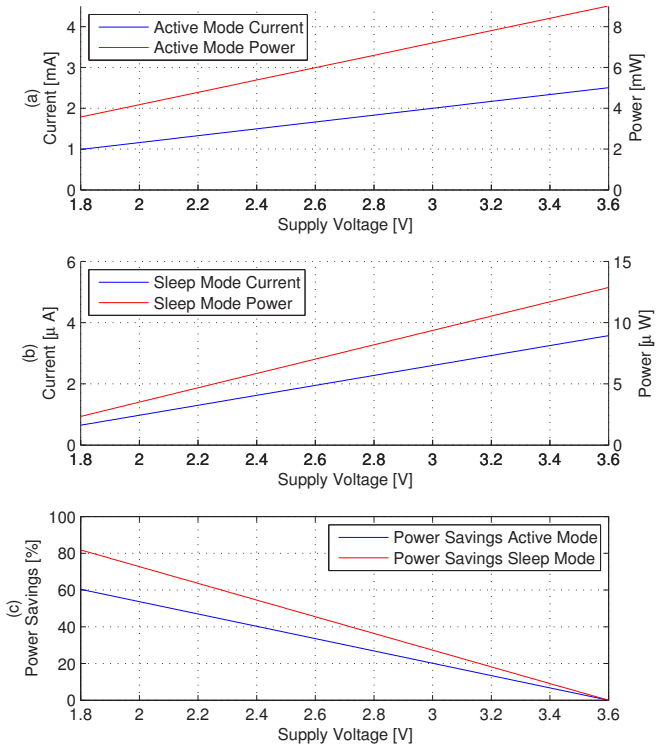

Fig. 4. Current and power consumption during active mode (a) and sleep mode (b) using a linear voltage regulator; (c) shows the theoretical power savings in active and sleep mode reffering to a supply voltage of 3.6 V.

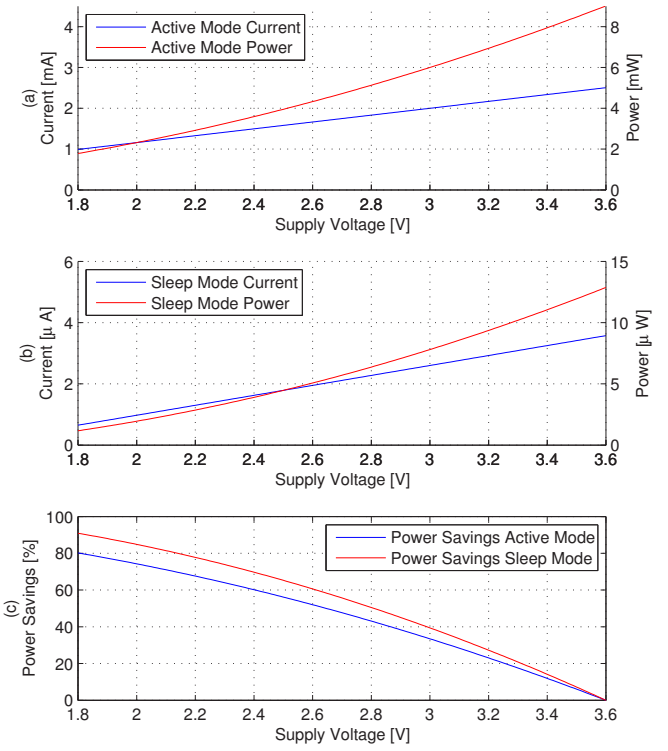

Fig. 5. Current and power consumption during active mode (a) and sleep mode (b) using a step down converter. (c) shows the theoretical power savings in active and sleep mode reffering to a supply voltage of 3.6 V.

that the sleep current depends also linear on the supply voltage the resulting power consumption has a linear dependency, too.

Finally, 4c shows the theoretical power savings using an LDO regulator. No losses are assumed here.

2) Step Down Converter: A step down converter, also called buck converter, provides a constant output voltage by using internal switching elements. Typically a coil or a capacitor is used in combination with the switches. The output voltage can be controlled by varying the timing of the switching elements (pulse-width modulation).

Figure 5a shows the dependency of the current (blue trace) and the power consumption (red trace) of the microcontroller depending on the supply voltage during active mode at 4 MHz. The values are simulated using Equation 2. When using a step down converter, the difference between the battery voltage V_{Bat} and the supply voltage of the microcontroller V_{CC} drops at the converter V_{Buck} (see Equation 11).

$$V_{Bat} = V_{StepDown} + V_{CC} \tag{11}$$

However, the average input current of the converter is unequal to the output current and therefore, it is different form the current through the microcontroller (Equation 12).

$$I_{Buck,input} \neq I_{Buck,output} = I_{\mu C} \tag{12}$$

The ideal step down converter has no losses and therefore, the input power of it is equal to the output power. This means that the input power depends only on the power consumption of the microcontroller as shown in Equation 13.

$$\begin{aligned} P_{IN}(V_{CC}) &= P_{OUT}(VCC) \\ &= I_{AM}(V_{CC}) \cdot V_{CC} \end{aligned} \tag{13}$$

It can be seen that the power consumption depends quadratically on the supply voltage. The reason is that the input current of the step down converter is lower than the output current.

Figure 5b shows the dependency of the current (blue trace) and the power consumption (red trace) of the microcontroller depending on the supply voltage during sleep mode (low power mode 3, only the 32 kHz timer is active). Due to the fact that the sleep current has the same influence on the power consumption, the power consumption depends quadratically on the supply voltage, too.

Finally, 5c shows the theoretical power savings using a step down converter. No losses are assumed here.

C. Component-Aware Dynamic Voltage Scaling

CADVS can be applied to reduce the power consumption of the hardware. As shown in Table III the minimum allowed supply voltage varies over the time. It is assumed that only a few messages are sent. Therefore, the energy of the transmissions is neglected at the following calculations. This can be done, because the main focus of this work is on the possible energy savings using CADVS and not on a correct energy estimation of an application running on the sensor node. Furthermore, it is

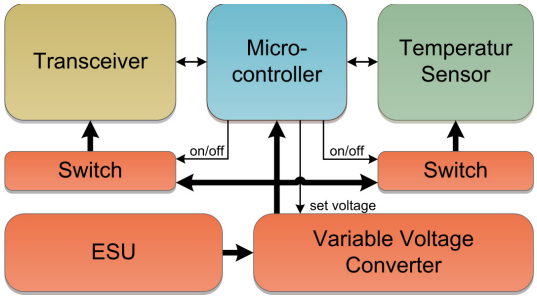

Fig. 6. Structure of the WSN node (extended from [21]). The power supply of the temperature sensor and of the transceiver can be switched off by the microcontroller. Furthermore, the variable voltage converter enables CADVS.

TABLE V
CURRENT CONSUMPTION OF THE COMPONENTS OF THE SENSOR NODE.

Component	Sleep	Active Measure	Active Computation	Active Commun.
V_{CC}	1.8 V	3.3 V	1.8 V	2.4 V
Microcontroller	650 nA	2.25 mA	0.992 mA	1.5 mA
Transceiver	0	0	0	25 mA
Temp. Sensor	0	0.37 mA	0	0
Power Switches	170 nA	402 nA	170 nA	259 nA
Sum	820 nA	2.62 mA	0.99 mA	26.5 mA

TABLE VI
POWER CONSUMPTION OF THE COMPONENTS OF THE SENSOR NODE.

Component	Sleep	Active Measure	Active Computation	Active Commun.
V_{CC}	1.8 V	3.3 V	1.8 V	2.4 V
Microcontroller	1170 nW	7.43 mW	1.786 mW	3.6 mW
Transceiver	0	0	0	60 mW
Temp. Sensor	0	1.221 mW	0	0
Power Switches	306 nW	1327 nW	306 nW	621 nW
Sum	1476 nW	8.65 mA	1.79 mW	63.6 mW

assumed that the transceiver and the temperature sensor can be switched off completely. This is necessary, because they have very high sleep currents (compared to the microcontroller). Fig. 6 shows the resulting block diagram of the sensor node. TPS22921 from Texas Instruments are assumed as power switches [28].

Table V and Table VI shows an overview of the current consumption and power consumption of the single components during the different subintervals.

As mentioned before, two different techniques can be used to convert the supply voltage of the WSN node. The following figures and tables show the possible power savings using an LDO regulator with fixed output voltage (3.3V), an LDO regulator with variable output voltage (CADVS), a step down converter with fixed output voltage (3.3 V) and a step down converter with variable output voltage (CADVS).

The voltage of the battery is assumed to be $V_{bat} = 3.77$ V. This is the mean of the average discharge voltages of the rechargeable batteries (see Table IV). The power savings are calculated using the LDO regulator with fixed output voltage as reference, because it is the simplest supply configuration. Table VII shows the power consumption and the theoretical

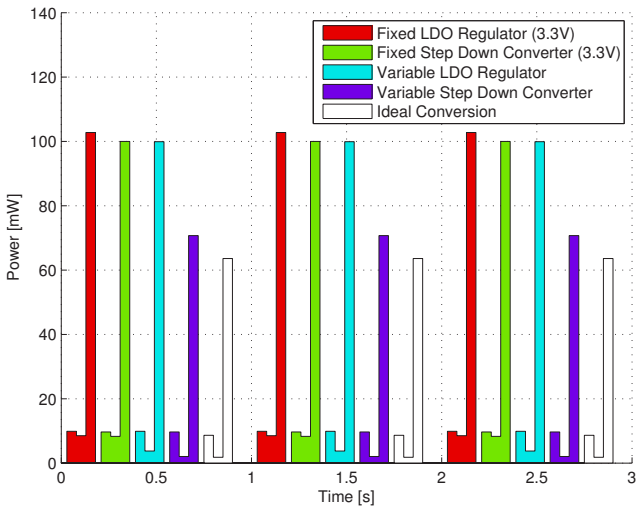

Fig. 7. Power consumption of the WSN node with four different supply configurations and ideal conversion.

power savings of the different subintervals using the four different supply configurations.

It is also important to consider the quiescent current of the voltage converters. The LDO regulator TPS78001 from Texas Instruments has a quiescent current of $I_{q,LDO} = 500$ nA [26]. The quiescent current of the step down converter TPS62120 also from Texas Instruments is $I_{q,stepdown} = 11\mu$A [25]. Furthermore, the efficiency of the TPS62120 is about 90 %. To adjust the output voltage a digital potentiometer is needed. The quiescent current of the ISL22313 from Intersil is $I_{q,dpot} = 1\,\mu$A [29]. The results of this calculation are shown in Table VIII.

Fig. 7 shows the power trace of the WSN node using the four different supply configurations. Three intervals are plotted. The white trace shows the minimum possiple supply power using ideal components without conversion losses and leakage currents.

The comparison of Table VII and Table VIII is very interesting. The best supply configuration of theoretical calculation (Table VII) is the variable step down converter. It is also the best supply configuration including the efficiency and the quiescent currents of the voltage converter. However, the energy savings of the variable step down converter drops significantly. The reason is the energy wasting of the step down converter during the sleep subinterval. Analyzing the savings during each subinterval, it can be seen that the step down converter has much higher power savings at higher power consumptions and lower supply voltages. The average power savings depends on the DC of the WSN node. This is shown in Fig. 8. Therefore, the sleep duration is varied and the durations of the active subintervals are kept constant. The shorter the sleep duration, the higher is the DC. It can be seen that at a higher DC the step down converter using CADVS provides the best results. At a lower DC, the LDO regulator using CADVS provides the best results. However,

TABLE VII
POWER CONSUMPTION AND THEORETICAL POWER SAVINGS OF THE FOUR DIFFERENT SUPPLY CONFIGURATIONS.

Description	Fixed LDO Reg. 3.3 V	Fixed Step Down Conv. 3.3 V	Variable LDO Reg.	Variable Step Down Conv.
Sleep Power	13.32 μW	11.66 μW	3.09 μW	1.48 μW
Measurement Power	9.89 mW	8.65 mW	9.89 mW	8.65 mW
Computation Power	8.49 mW	7.43 mW	3.74 mW	1.79 mW
Communication Power	102.74 mW	89.93 mW	99.89 mW	63.59 mW
Average Power	6.07 mW	5.31 mW	5.68 mW	3.70 mW
Sleep Power Savings	0.0 %	12.5 %	76.8 %	88.9 %
Measurement Power Savings	0.0 %	12.5 %	0.0 %	12.5 %
Computation Power Savings	0.0 %	12.5 %	56.0 %	79.0 %
Communication Power Savings	0.0 %	12.5 %	2.8 %	38.1 %
Average Power Savings	0.0 %	12.5 %	6.4 %	39.0 %

TABLE VIII
POWER CONSUMPTION AND POWER SAVINGS OF THE FOUR DIFFERENT SUPPLY CONFIGURATIONS INCLUDING THE QUIESCENT CURRENT OF THE VOLTAGE CONVERTER.

Description	Fixed LDO Reg. 3.3 V	Fixed Step Down Conv. 3.3 V	Variable LDO Reg.	Variable Step Down Conv.
Quiescent Current Voltage Conv.	0.5 μA	11.0 μA	1.5 μA	12.0 μA
Quiescent Power Voltage Conv.	1.9 μW	41.5 μW	5.7 μW	45.2 μW
Sleep Power	15.20 μW	54.42 μW	8.75 μW	46.88 μW
Measurement Power	9.89 mW	9.66 mW	9.89 mW	9.66 mW
Computation Power	8.49 mW	8.30 mW	3.75 mW	2.03 mW
Communication Power	102.74 mW	99.97 mW	99.90 mW	70.70 mW
Average Power	6.07 mW	5.94 mW	5.68 mW	4.16 mW
Sleep Power Savings	0.0 %	−258.0 %	42.5 %	−208.4 %
Measurement Power Savings	0.0 %	2.3 %	−0.0 %	2.3 %
Computation Power Savings	0.0 %	2.3 %	55.9 %	76.1 %
Communication Power Savings	0.0 %	2.7 %	2.8 %	31.2 %
Average Power Savings	0.0 %	2.1 %	6.3 %	31.5 %

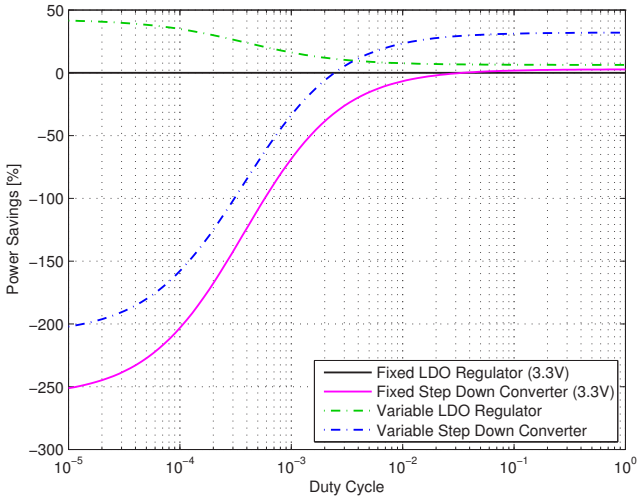

Fig. 8. Power savings of the WSN node depending on the DC.

there are applications with a dynamic DC. This means the DC is adapted to the current circumstances. The best solution is to combine an LDO regulator and a step down converter. Only the voltage converter with the better power savings is active.

IV. EVALUATION

This section evaluates the results of the previous sections. Unfortunately, no fully functional prototype was available to perform a complete evaluation. However, the current consumption of the transceiver and of the microprocessor was measured. Fig. 9 shows the current consumption of the transceiver depending on the supply voltage during receiving.

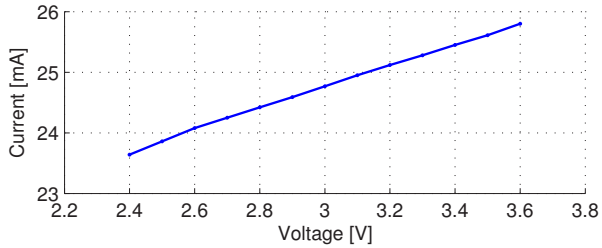

Fig. 9. Current consumption of the transceiver depending on the supply voltage.

Fig. 10 shows the active current consumption of the MSP430F1611 microprocessor. The active mode current is similar to the current specified in the datasheet. It can be seen that the difference of the lowest and the highest current of the transceiver is smaller than the difference of the microcontroller. Furthermore, the measurements have shown that the assumption of the linear dependency of the current consumption on the supply voltage is acceptable.

V. CONCLUSION AND FUTURE WORK

This work demonstrated different possibilities of the supply of WSN nodes. It has shown different voltage conversion

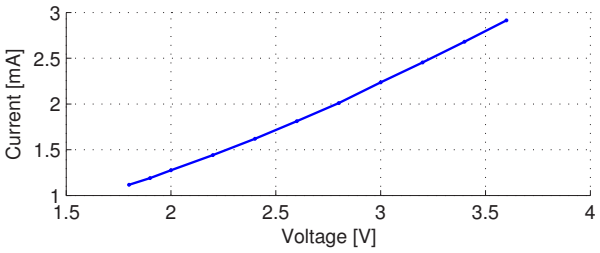

Fig. 10. Active mode current consumption of the MSP430F1611 depending on the supply voltage.

techniques and their advantages and disadvantages concerning the energy savings. A realistic scenario has been developed to show how DVS can be used to save up to 31.5 % of the energy compared to a constant voltage supply using the introduced scenario while achieving the same end-user performance. Furthermore, it demonstrated the energy savings dependent on the DC of a WSN node considering the leakage currents and the conversion efficiency of the four different voltage conversion techniques. Finally, two measurements have shown that the assumptions of a linear dependency of the current consumption on the supply voltage are acceptable. Future activities will target an implementation of a prototype to evaluate the different voltage conversion techniques with real components.

REFERENCES

[1] R. Min, M. Bhardwaj, S.-H. Cho, N. Ickes, E. Shih, A. Sinha, A. Wang, and A. Chandrakasan, "Energy-centric enabling tecumologies for wireless sensor networks," *Wireless Communications, IEEE*, vol. 9, no. 4, pp. 28 – 39, aug. 2002.

[2] V. Raghunathan, A. Kansal, J. Hsu, J. Friedman, and M. Srivastava, "Design considerations for solar energy harvesting wireless embedded systems," in *Proceedings of the 4th international symposium on Information processing in sensor networks*. IEEE Press, 2005, p. 64.

[3] M. Rahimi, H. Shah, G. Sukhatme, J. Heideman, and D. Estrin, "Studying the feasibility of energy harvesting in a mobile sensor network," *Robotics and Automation, 2003. Proceedings. ICRA '03. IEEE International Conference on*, vol. 1, pp. 19 – 24 vol.1, sep. 2003.

[4] A. Janek, C. Trummer, C. Steger, R. Weiss, J. Preishuber-Pfluegl, and M. Pistauer, "Simulation based verification of energy storage architectures for higher class tags supported by energy harvesting devices," *Microprocessors and Microsystems*, vol. 32, no. 5-6, pp. 330–339, 2008, dependability and Testing of Modern Digital Systems. [Online]. Available: http://www.sciencedirect.com/science/article/B6V0X-4S80XHN-2/2/22459f6e78fe4b7c4111c8af88fa7fb4

[5] K. Langendoen, A. Baggio, and O. Visser, "Murphy loves potatoes: experiences from a pilot sensor network deployment in precision agriculture," *Parallel and Distributed Processing Symposium, 2006. IPDPS 2006. 20th International*, p. 8 pp., apr. 2006.

[6] N. Watthanawisuth, A. Tuantranont, and T. Kerdcharoen, "Microclimate real-time monitoring based on zigbee sensor network," *Sensors, 2009 IEEE*, pp. 1814 –1818, oct. 2009.

[7] P. Juang, H. Oki, Y. Wang, M. Martonosi, L. S. Peh, and D. Rubenstein, "Energy-efficient computing for wildlife tracking: design tradeoffs and early experiences with zebranet," in *ASPLOS-X: Proceedings of the 10th international conference on Architectural support for programming languages and operating systems*. New York, NY, USA: ACM, 2002, pp. 96–107.

[8] A. Lindgren, C. Mascolo, M. Lonergan, and B. McConnell, "Seal-2-seal: A delay-tolerant protocol for contact logging in wildlife monitoring sensor networks," *Mobile Ad Hoc and Sensor Systems, 2008. MASS 2008. 5th IEEE International Conference on*, pp. 321 –327, sep. 2008.

[9] K. Lorincz, B.-r. Chen, G. W. Challen, A. R. Chowdhury, S. Patel, P. Bonato, and M. Welsh, "Mercury: a wearable sensor network platform for high-fidelity motion analysis," in *SenSys '09: Proceedings of the 7th ACM Conference on Embedded Networked Sensor Systems*. New York, NY, USA: ACM, 2009, pp. 183–196.

[10] N. Xu, S. Rangwala, K. K. Chintalapudi, D. Ganesan, A. Broad, R. Govindan, and D. Estrin, "A wireless sensor network for structural monitoring," in *SenSys '04: Proceedings of the 2nd international conference on Embedded networked sensor systems*. New York, NY, USA: ACM, 2004, pp. 13–24.

[11] C. Enz, N. Scolari, and U. Yodprasit, "Ultra Low-Power Radio Design for Wireless Sensor Networks," in *IEEE Int. Workshop on Radio-Frequency Integration Technology*, 2005, pp. 1–17, (Invited Keynote).

[12] M. Minami, T. Morito, H. Morikawa, and T. Aoyama, "Solar biscuit: A battery-less wireless sensor network system for environmental monitoring applications," *The 2nd International Workshop on Networked Sensing Systems*, 2005.

[13] A. Kansal, D. Potter, and M. B. Srivastava, "Performance aware tasking for environmentally powered sensor networks," in *SIGMETRICS '04/Performance '04: Proceedings of the joint international conference on Measurement and modeling of computer systems*. New York, NY, USA: ACM, 2004, pp. 223–234.

[14] P. He, Q. Cui, and X. Guo, "Efficient solar power scavenging and utilization in mobile electronics system," *Green Circuits and Systems (ICGCS), 2010 International Conference on*, pp. 641 –645, jun. 2010.

[15] S. Roundy, D. Steingart, L. Frechette, P. Wright, and J. Rabaey, "Power sources for wireless sensor networks," in *Wireless Sensor Networks*, ser. Lecture Notes in Computer Science. Springer Berlin / Heidelberg, 2004, vol. 2920, pp. 1–17.

[16] T. D. Burd and R. W. Brodersen, "Design issues for dynamic voltage scaling," in *Proceedings of the 2000 international symposium on Low power electronics and design*, ser. ISLPED '00. New York, NY, USA: ACM, 2000, pp. 9–14. [Online]. Available: http://doi.acm.org/10.1145/344166.344181

[17] T. Simunic, L. Benini, A. Acquaviva, P. Glynn, and G. De Micheli, "Dynamic voltage scaling and power management for portable systems," in *Proceedings of the 38th annual Design Automation Conference*, ser. DAC '01. New York, NY, USA: ACM, 2001, pp. 524–529. [Online]. Available: http://doi.acm.org/10.1145/378239.379016

[18] J. Pouwelse, K. Langendoen, and H. Sips, "Dynamic voltage scaling on a low-power microprocessor," in *Proceedings of the 7th annual international conference on Mobile computing and networking*, ser. MobiCom '01. New York, NY, USA: ACM, 2001, pp. 251–259. [Online]. Available: http://doi.acm.org/10.1145/381677.381701

[19] A. Sinha and A. Chandrakasan, "Dynamic power management in wireless sensor networks," *Design Test of Computers, IEEE*, vol. 18, no. 2, pp. 62 –74, Mar./Apr. 2001.

[20] H. C. Powell, A. T. Barth, and J. Lach, "Dynamic voltage-frequency scaling in body area sensor networks using cots components," in *Proceedings of the Fourth International Conference on Body Area Networks*, ser. BodyNets '09. ICST, Brussels, Belgium, Belgium: ICST (Institute for Computer Sciences, Social-Informatics and Telecommunications Engineering), 2009, pp. 15:1–15:8. [Online]. Available: http://dx.doi.org/10.4108/ICST.BODYNETS2009.6015

[21] D. Puccinelli and M. Haenggi, "Wireless sensor networks: applications and challenges of ubiquitous sensing," *Circuits and Systems Magazine, IEEE*, vol. 5, no. 3, pp. 19–31, 2005.

[22] TexasInstruments, "Msp430f15x, msp430f16x, msp430f161x mixed signal microcontroller," www.focus-ti.com, SLAS368F, 2009.

[23] AnalogDevices, "$\pm 0.5^{\circ}$C accurate pwm temperature sensor in 5-lead sc-70," www.analog.com, D03340 Rev.B, 2006.

[24] Microchip, "Mrf24j40mb data sheet - 2.4 ghz ieee std. 802.15.4 20 dbm rf transceiver module," www.microchip.com, DS70599B, 2009.

[25] TexasInstruments, "Tps62120 - 15V, 75mA high efficient buck converter," www.focus-ti.com, SLVSAD5, July 2010.

[26] ——, "Tps780 series - 150mA, low-dropout regulator, ultralow-power, i_q 500nA with pin-selectable, dual-level output voltage," www.focus-ti.com, SLVSAD5, May 2008.

[27] D. Linden and T. B. Reddy, *Handbook of Batteries*, 3rd ed. New York: McGraw-Hill, 2002.

[28] TexasInstruments, "Tps22921 - low input voltage, ultra-low r_{ON} load switches," www.focus-ti.com, SLVS749A, December 2008.

[29] Intersil, "Isl22313 - single digitally controlled potentiometer (xdcp(tm))," www.intersil.com, FN6421.0, July 2007.